Confinement effects on glass forming liquids probed by dynamic mechanical analysis

J. Koppensteiner,* W. Schranz,† and M. R. Puica‡
Faculty of Physics, University of Vienna, Boltzmanngasse 5, A-1090 Vienna, Austria
(Received 12 June 2008; revised manuscript received 30 July 2008; published 26 August 2008)

Many molecular glass forming liquids show a shift of the glass transition T_g to lower temperatures when the liquid is confined into mesoporous host matrices. Two contrary explanations for this effect are given in literature: First, confinement induced acceleration of the dynamics of the molecules leads to an effective downshift of T_g increasing with decreasing pore size. Second, due to thermal mismatch between the liquid and the surrounding host matrix, negative pressure develops inside the pores with decreasing temperature, which also shifts T_g to lower temperatures. Here we present dynamic mechanical analysis measurements of the glass forming liquid salol in Vycor and Gelsil with pore sizes of d=2.6, 5.0 and 7.5 nm. The dynamic complex elastic susceptibility data can be consistently described with the assumption of two relaxation processes inside the pores: A surface induced slowed down relaxation due to interaction with rough pore interfaces and a second relaxation within the core of the pores. This core relaxation time is reduced with decreasing pore size d, leading to a downshift of $T_g \propto 1/d$ in perfect agreement with recent differential scanning calorimetry (DSC) measurements. Thermal expansion measurements of empty and salol filled mesoporous samples revealed that the contribution of negative pressure to the downshift of T_g is small ($<30\%$) and the main effect is due to the suppression of dynamically correlated regions of size ξ when the pore size d approaches ξ.

DOI: 10.1103/PhysRevB.78.054203 PACS number(s): 64.70.pm, 61.20.Lc, 62.25.−g

I. INTRODUCTION

When approaching a glass transition some physical properties like viscosity or relaxation times change up to 14 orders of magnitude.[1,2] An explanation for the observed slowing down of the dynamics is the formation of collectively dynamically rearranging clusters[3,4] or regions, with growing size ξ and increasing relaxation times as T_g is approached.[5] The idea of an increasing dynamic correlation length ξ when approaching a glass transition is strongly supported by recent computer simulations,[6–8] although not strictly proven, since computer simulations cannot treat the time range of the α-process. Very recently a breakthrough was achieved in this field. Biroli *et al.*[9] found first-time evidence that the mode coupling theory predicts a growing dynamic length scale approaching the glass transition of a supercooled liquid. The authors obtained a rather modest growth of the dynamical length scale ξ with decreasing temperature, which is in very good agreement with computer simulations[8] and experimental results. Indeed many experimental setups like heat capacity spectroscopy,[10,11] multidimensional NMR,[12–14] multipoint dynamical susceptibilities,[15] etc. have been used to monitor a possible growing length scale accompanying the glass transition. All these results agree in the fact that the obtained dynamically correlated regions—although material dependent—are on the order of 1–4 nm and display—if at all—a weak temperature dependence.

An alternative experimental approach to get a reference to a possibly existing cooperation length ξ which increases when $T \to T_g$ is by spatial limitation of a glass forming liquid. Spatially confining geometries as ultrathin films, mesoporous silica or zeolithes have already been used to study phase transitions of water,[16] hydrocarbons,[17] noble gases,[18,19] liquid crystals[20] or alkenes.[21] But this concept also illuminated the old and still open question on the very nature of the glass transition and its dynamics:[22] In a pioneering work Jackson and McKenna[23] studied the glass transition of organic liquids in controlled pore glasses (CPG) for various pore sizes d. They found a reduction of the glass transition temperature T_g for liquids in confinement as compared to the bulk material. The downshift of T_g was larger for smaller pore sizes, i.e., $\Delta T_g \propto 1/d$, an effect similar but not as strong as the suppression known for the melting temperature T_m in confinement. During the following two decades this effect was studied via calorimetry,[24,25] dielectric spectroscopy,[26] neutron scattering,[27] light scattering,[28] and molecular dynamics.[29] It was shown that in many cases confinement below a characteristic length impedes[24] the transition, implying that molecules within a region of the size ξ_g (approaching T_g typically some nm[30,31]) have to cooperate and rearrange in order to create the glassy state. Hindering this cooperation first leads to a downshift of T_g if $d \sim \xi_g$ and finally to a suppression of the transition if $d < \xi_g$.[24]

However, although this shift of T_g with decreasing confinement size was found in numerous studies, there are complications which blur this simple picture: e.g., in many molecular dynamics simulations of glass forming liquids at high temperatures above the empirical mode-coupling temperature T_c confinement is found to slow down the dynamics.[32,33] Furthermore, in some systems a competition appears between slowing down of molecular motions due to pinning of the molecules at the pore surface and acceleration of the dynamics due to decreasing size of the confinement. Another effect occurs due to the difference in thermal expansion coefficients of the porous host matrix and the glass forming liquid. This may create negative pressure upon the confined liquid when the glass transition is approached. Some authors attribute the whole observed downshift of T_g to this negative pressure effect.[28] We will address these points in more detail below. For excellent reviews about these topics the reader is referred to Refs. 34 and 35.

Very recently the confinement effect on the glass forming liquid salol was studied via dynamic mechanic analysis

TABLE I. N_2 adsorption characteristics of porous silica samples.

	Gelsil 2.6	Gelsil 5	Vycor
Av. pore diameter (nm)	2.6	5.0	7.5
Surface area (m^2/g)	586	509	72
Pore volume (cm^3/g)	0.376	0.678	0.214
Porosity ϕ	0.51	0.66	0.30

(DMA)[36] measurements in Vycor with $d=7$ nm pore size. It turned out that the dynamic elastic response is very sensitive to the glass transition of liquids confined to mesoporous samples. Based on the results of computer simulations[29,37] we could disentangle acceleration effects due to confinement and slowing down of molecular motion due to interaction of the molecules with the rough pore surface. We could even predict the pore size dependence of the dynamic elastic response (see Fig. 4 of Ref. 36). In order to test these predictions and to study the glass transition of salol for different pore sizes, further measurements have been performed. Here we present experimental results of the temperature and frequency dependence of the complex dynamic elastic susceptibility of salol confined in mesoporous matrices of $d=7.5$, 5.0, and 2.6 nm. In addition, thermal expansion measurements have been performed, which now allows us to take a new look at the often discussed negative pressure effect on glass forming liquids in confinement and to separate this effect from an intrinsic size effect.

The present paper is organized as follows: Sec. II yields insight into sample preparation and some technical details of DMA analysis. Section III displays a compilation of the experimental data and results of modeling and interpretation of the present data. It also contains a calculation of the effect of adsorption swelling and the separation of the actual downshift of T_g in salol into the negative pressure effect and the confinement effect. Section IV concludes the paper.

II. EXPERIMENT

A. Sample preparation

Porous Vycor samples are made by Corning Inc., NY and sold under the brand name "Vycor 7930." Via phase separation and leaching a three-dimensional random network of pores in nearly pure silica is fabricated.[38] Pores are uniformly distributed in length, direction, and density.[39] The mean ratio of average pore diameter d and pore length l is $d/l \approx 0.23$. Gelsil is a mesoporous xerogel consisting of pure silica with a very narrow pore radius distribution. Gelsil rods were made by 4F International Co., Gainesville, FL. Results on pore sizes were derived from Barrett-Joyner-Halenda (BJH) analysis of the individual N_2-desorption isotherms[40] and are summarized in Table I.

All samples were cut and sanded in order to gain parallel surface plains. The typical size of a sample was $(2\times2\times8)$ mm^3 for parallel plate and about $(2\times1\times7)$ mm^3 for three-point-bending DMA measurements. Cleaning was done in a 30% hydrogen peroxide solution at 90 °C for 24 h, drying at 120 °C in a high-vacuum chamber at 10^{-6} bar, also for about 24 h. The guest glass forming material was salol (phenyl salicylate, $C_{13}H_{10}O_3$), a low molecular weight liquid, whose melting temperature is $T_m=316$ K. Salol is a standard, so-called fragile,[41] glass former ($m=73$) known[25] to form a glass either at extreme cooling rates of 500 K/min or in pores smaller than 11.8 nm. Filling was done at 317 K via capillarity wetting. By comparing the weight of clean and filled samples the filling fractions f were determined (see Table III).

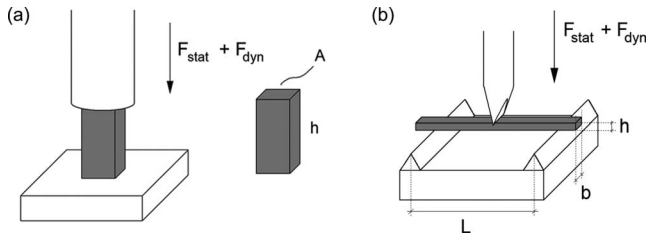

FIG. 1. Sketch of (a) parallel plate and (b) three-point-bending geometry.

B. Dynamic mechanical analysis

In this method a static and a dynamic force $F_{stat}+F_{dyn}\cdot e^{i\omega t}$ (0.001–16 N at 0.01–100 Hz) are applied on a sample using a quartz or steel rod (see Fig. 1). The response of the sample is measured via the displacement of the rod. Absolute height h, height amplitude Δh, and phase lag δ are read via electromagnetic inductive coupling (LVDT) with a resolution of 10 nm and 0.01°, respectively. These data allow direct access to real and imaginary parts of the complex elastic susceptibility at low frequency and as a function of temperature and applied force. In addition, the thermal expansion of a sample can be determined in the so-called thermo mechanical analysis (TMA) mode, where no external force is applied. Two devices are used: A DMA 7 and a Diamond DMA, both from Perkin Elmer Inc. Two measuring geometries are applied: Parallel plate (PP) compression and three-point bending (3PB) (see Fig. 1).

Parallel plate geometry reveals purely the complex Young's modulus $Y^*=Y'+iY''$, where Y' and Y'' are the storage and the loss modulus, respectively. The three-point-bending geometry delivers Young's modulus plus a small (geometry dependent) contribution of a shear elastic constant. More details on measurement geometry may be found in Refs. 42 and 43. The absolute accuracy of resulting real and imaginary parts Y' and Y'' is rather poor, mainly because of contact losses between the quartz rod and the sample. A discussion of these systematic errors may be found in Ref. 36. In contrast the relative accuracy is excellent and the DMA method is estimated to be about 100 times more sensitive to detect glass transitions or other subtle phase transitions than differential scanning calorimetry (DSC) measurements.[44]

III. RESULTS AND DISCUSSION

A. Dynamic elastic response

Diamond DMA measurements (in parallel plate and three-point-bending geometry) of Vycor and Gelsil samples filled

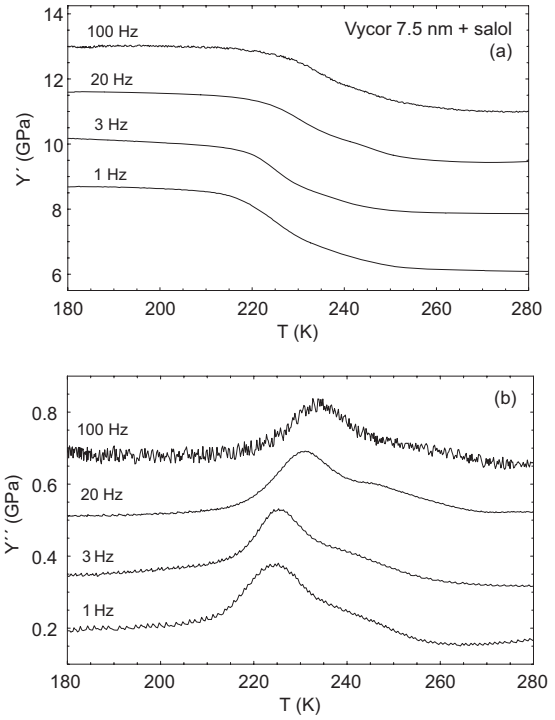

FIG. 2. Real (a) and imaginary parts (b) of the complex Young's modulus of Vycor 7.5 nm filled with salol (filling fraction $f \approx 0.79$) measured in three-point-bending geometry. The curves are offset from the 1 Hz data for sake of clarity.

with salol are shown in Figs. 2–5. The loss modulus Y'' [Fig. 2(b)] of salol in 7.5 nm pores clearly shows a "two-peak structure," i.e., a peak with half-width at half maximum (HWHM) about 20 K, and a shoulder or second peak at about 15 K higher temperature [also see Fig. 5(b)]. This is also reflected by the real part Y', which displays a "two-step-like shape" with temperature [Figs. 2(a) and 5(a)]. Both peaks in Y'' shift to higher temperatures with increasing frequency as expected for a glass transition. In smaller pores of Gelsil 5.0, peak and shoulder merge into one asymmetric peak of width ~30 K [see Figs. 3(b) and 5(e)], also shifted with higher frequency to higher temperatures. In 2.6 nm pores the loss peak shows a rather symmetric form broadened up to about 60 K [see Figs. 4(b) and 5(f)].

While in large pores of 7.5 nm diameter vitrification of salol seems to happen decoupled (two peaks in Y'') in regions near the pore surface and the pore center; things change in smaller pores. With decreasing pore diameter, Y'' approaches a symmetric form and simultaneously Y' changes from a "double step shape" into a "single step shape," indicating only one type of relaxation process. Similar broadening effects as for the loss peaks of our DMA measurements were observed in pores of decreasing size also by calorimetric[23] and dielectric measurements.[45,46] This broadening as well as a shift of the glass transition to lower temperatures was calculated by Sappelt and Jäckle[47] using kinetic Ising and lattice gas models, and shown to originate from confinement induced suppression of cooperative motion of molecules.

Pure Vycor and Gelsil, meaning exposed to air and therefore mostly filled with nitrogen, do not show any of these features. Y' decreases about 2% between 300 and 180 K. Y''

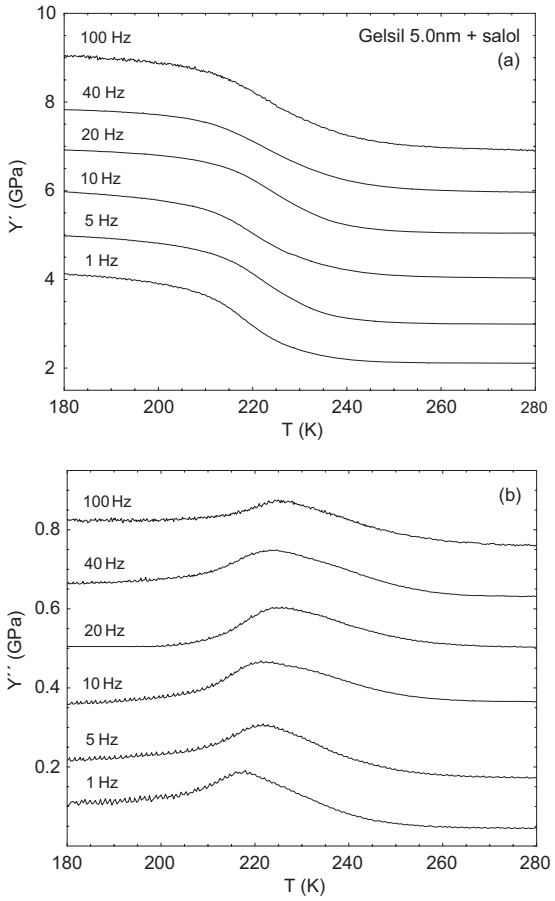

FIG. 3. Real (a) and imaginary (b) parts of the complex Young's modulus of Gelsil 5.0 nm filled with salol (filling fraction $f \approx 0.75$) measured in parallel plate geometry (Diamond DMA). The 1 Hz signal is original data; other signals are offset for sake of clarity.

is constant within the corresponding temperature range.

Any standard relaxation model like Debye, Kohlrausch, Cole-Cole or Cole-Davidson fails to describe our dynamic elastic susceptibility data if only one type of relaxation process is assumed. One would have to use extreme stretching parameters to fit Y', which then leads to improper temperature shifts of the peaks in Y'' with respect to the experimental data and misfitting signal heights. The most efficient model to describe our data turned out to be a modification of the empirical Vogel-Fulcher-Tammann law

$$\tau(T) = \tau_0 \cdot \exp\left[\frac{E}{T - T_0}\right], \tag{1}$$

where τ_0 is a preexponential factor, $E \cdot k_B$ is an activation energy, and T_0 is the Vogel-Fulcher (VF) temperature. Following computer simulations[29,37] we take into account a shift of VF temperatures along the pore radius r. In a recent paper Zorn *et al.*[27] suggest the empirical ansatz

$$T_0(r) = T_{00} + \frac{k}{R - r + r_p}, \tag{2}$$

with the bulk VF temperature T_{00}, and the pore radius $R = d/2$. The so-called penetration radius r_p is the radius be-

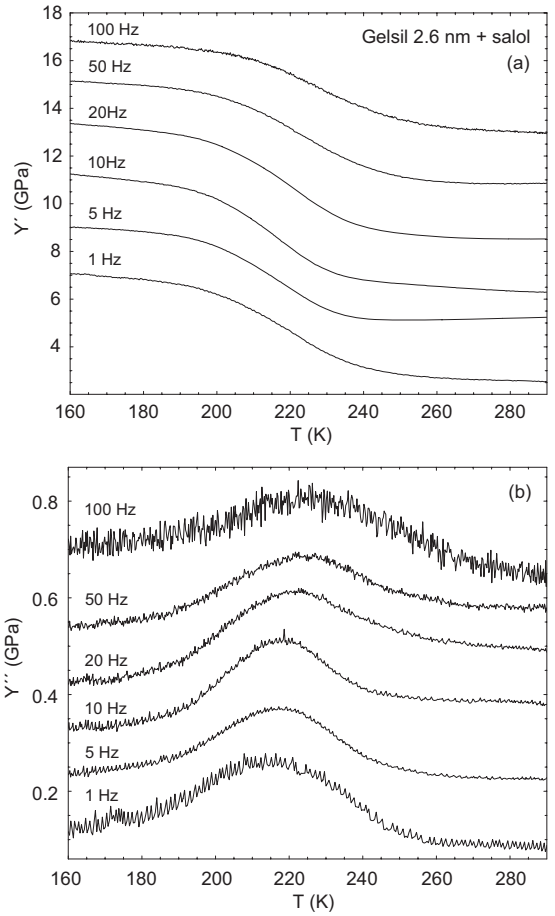

FIG. 4. Real (a) and imaginary (b) parts of the complex Young's modulus of Gelsil 2.6 nm filled with salol (filling fraction $f \approx 0.65$) measured in three-point-bending geometry (Diamond DMA). The 1 Hz signal is original data; other signals are offset for sake of clarity.

yond which it is very unlikely to find a particle in the fluid state.[29] The combination of Eqs. (1) and (2) leads to a radial distribution of relaxation times τ inside the pore:

$$\tau(r,T) = \tau_0 \cdot \exp\left[\frac{E}{T - \left(T_{00} + \frac{k}{R - r + r_p}\right)}\right]. \tag{3}$$

Equation (3) describes the exponential increase in relaxation time when a rough pore wall is approached, and a growing influence of the pore wall with decreasing temperature, a behavior which was also found by recent computer simulations.[8,29,37,48] A temperature parametrized Cole-Cole plot of Y'' vs Y' of our data calls for a Cole-Davidson model of the complex dynamic elastic susceptibility

$$Y^*(\omega) \propto \frac{1}{(1 + i\omega\tau)^{\gamma/2}}, \tag{4}$$

with $\omega = 2\pi\nu$, ν being the measurement frequency, and the broadening parameter γ. Using Eq. (3), averaging over the pore radius R, and separating real and imaginary part of $Y^* = Y' + i \cdot Y''$ by common procedures leads to

$$Y' = 1 - \frac{2\Delta Y}{R^2} \int_0^R \frac{\cos[\gamma \cdot \arctan(\omega\tau(r,T))]}{[1 + \omega^2\tau(r,T)^2]^{\gamma/2}} r dr, \tag{5a}$$

$$Y'' = \frac{2\Delta Y}{R^2} \int_0^R \frac{\sin[\gamma \cdot \arctan(\omega\tau(r,T))]}{[1 + \omega^2\tau(r,T)^2]^{\gamma/2}} r dr. \tag{5b}$$

As already mentioned above, the two-peak structure in Y'' of 7.5 and 5 nm confined salol (Figs. 2 and 3) suggests to split the dynamic elastic response into a core and a surface contribution: The molecules in the core (center of the pores) behave bulklike and are dynamically decoupled from the molecules near the pore surface. This is modeled by inserting into Eqs. (5a) and (5b) the corresponding relaxation times $\tau_0 \cdot \exp[E/(T - T_0)]$ given by Eq. (1) if $r \leq R_c$ and $\tau(r,T)$ given by Eq. (3) if $r > R_c$ (see also Fig. 7). The sum of the two contributions perfectly describes our Y' and Y'' data on

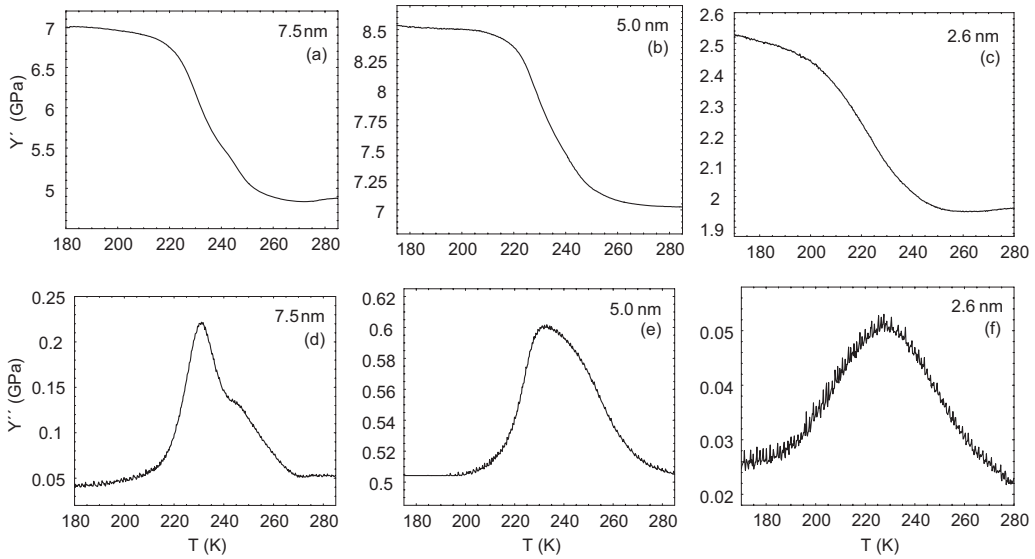

FIG. 5. Real (a) and imaginary (b) parts of the complex Young's modulus of salol in Vycor or Gelsil for different pore sizes, all measured at 20 Hz.

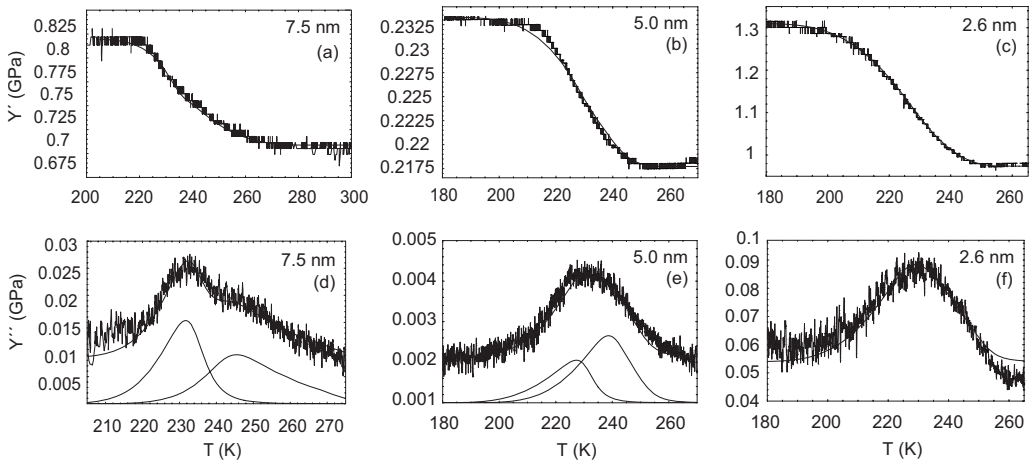

FIG. 6. Real part Y' and imaginary part Y'' of different porous samples filled with salol. The lines are fits using Eqs. (5a) and (5b) with parameters of Table II.

salol in 7.5 and 5 nm pores simultaneously (see Fig. 6).

In 2.6 nm pores we do not expect any molecule to behave like the bulk liquid any more, since the pore radius is of the same order as the estimated surface shell (see Table II), implying that every molecule is influenced by the near surface. Therefore we use Eqs. (5a) and (5b) with no bulk term which reproduces one single peak and also fits our data very well [Figs. 5(c) and 5(f) and Figs. 6(c) and 6(f)].

The radius of the "core" of bulklike interacting molecules turned out to be $R_c=2.5$ nm and 1.35 nm in 7.5 nm and 5.0 nm pores, respectively (see Table II). This implies that the thickness of the shell of molecules being slowed down by wall interaction $R-R_c=1.25$ nm and 1.15 nm for 7.5 nm and 5.0 nm pores, respectively.

Additional loss peaks, attributed to molecules forming H bonds to the inner pore surface, have also been reported from dielectric measurements of salol in 7.5 nm pores.[49,50] The work of Kremer and Stannarius[50] also revealed that the typical size of a shell of molecules interacting with the pore surface is about 2 or 3 molecules. Since the size of a salol molecule is estimated as $(1.4\times0.6\times0.4)$ nm^3 in Ref. 51 or as 0.282 nm^3 in Ref. 52, both corresponding to a mean diameter of 0.8 nm, this shell size is on the order of 1.6 to 2.4 nm. This is in very good agreement with our findings (see Table II). The core size R_c decreases with decreasing pore radius (see Table II and Fig. 7), also in very good agreement with the results of Kremer *et al.*[26]

The fitted Vogel-Fulcher temperature T_{00} is reduced with respect to the bulk and with decreasing pore size (see Table II). In order to compare our results with published data, we plotted the relaxation time in the pore center $\tau(r=0,T)$ for various pore sizes d and determined the corresponding $T_g(d)$ by using the common procedure[53] for finding the laboratory glass transition temperature, i.e., a cut with a horizontal line at $\tau=100$ s (see Fig. 8). As shown in Fig. 11, this leads to glass transition temperatures decreasing $\propto 1/d$ in very good agreement with published data of DSC measurements.[28]

On the other hand there are molecular dynamics simulations[32,33] of glass forming liquids pointing to the fact that at higher temperatures above the mode coupling temperature $T_c=260$ K of salol[54] confinement slows down the dynamics. However within the present experimental frequency range (0.01–100 Hz) we are not able to detect such a crossover to confinement induced slowing down by heating the sample from T_g to temperatures above T_c for the following reason: An extrapolation of the relaxation times of Fig. 8 to these temperatures shows that $\tau(T>260\ \text{K})<10^{-4}$ s, implying that $\omega\tau<1$ within this temperature range even at the

TABLE II. Fit parameters used in Eqs. (5a) and (5b) for fits of Fig. 6.

	Vycor	Gelsil 5	Gelsil 2.6
R (nm)	3.75	2.50	1.28
r_p (nm)	0.36	0.25	0.28
E (K)	1750	1750	1750
T_{00} (K)	158.5	156.2	136.0
τ_0 (s)	10^{-11}	10^{-11}	10^{-11}
γ	0.33	0.18	0.15
k (nm K)	18	11	25
R_c (nm)	2.5	1.35	
Shell $R-R_c$ (nm)	1.25	1.15	1.28

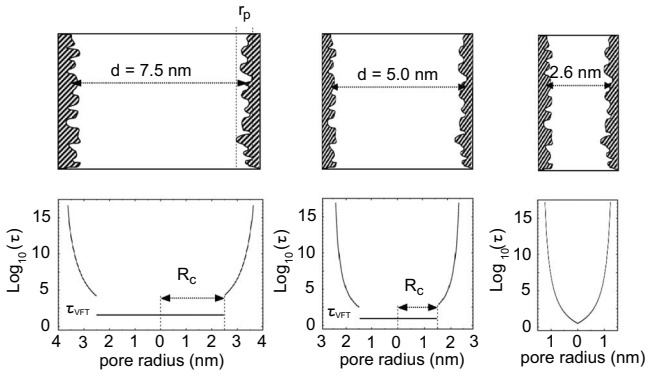

FIG. 7. Modeled relaxation time distributions in pores of diameter 7.5 nm to 2.6 nm from Eq. (3) used in Eqs. (5a) and (5b) for fits of Fig. 6.

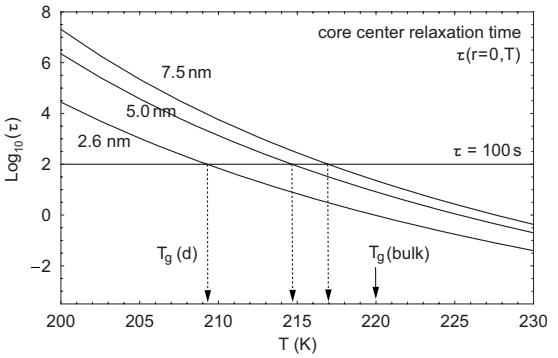

FIG. 8. Relaxation time in pore centers calculated from Eqs. (1) and (3) with corresponding parameters from Table II. The horizontal line shows $\tau=100$ s.

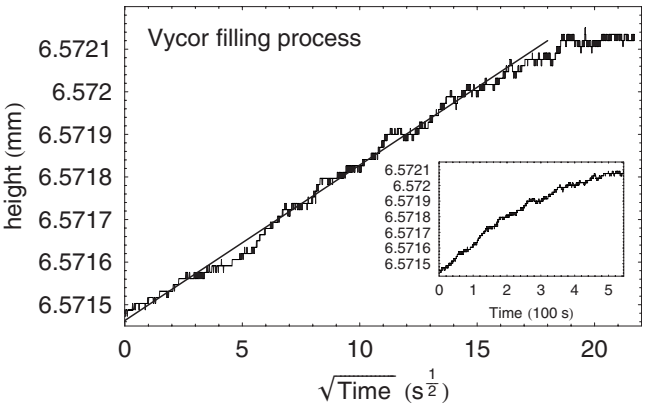

FIG. 9. Height of Vycor sample during the filling process against $\sqrt{t}$. The inset shows sample height against time.

highest available measurement frequency of 100 Hz. Therefore the dynamic elastic susceptibility given by Eq. (4) is actually independent of τ and we have to extend our frequency range to higher frequencies. Work in this direction using resonant ultrasound spectroscopy (RUS, 50 kHz$<\nu<$1.5 MHz) is in progress.

B. Filling process and accompanying effects

By using a DMA in a static TMA mode one can detect small changes in a sample's height with a resolution of 10 nm. We measured the time dependent swelling of the Vycor and Gelsil samples during filling with salol and the thermal expansion of empty and filled samples in the following way: In parallel plate mode, the quartz rod is placed on top of the sample with force $F=0$ N, and just height and temperature signals are read out. A clean piece of Vycor/Gelsil sample is cooled down to 170 K. Afterwards the sample is heated slightly above the melting temperature $T_m=316$ K of salol and kept there isothermally. Crystalline, powderlike salol placed right around the sample melts and percolates the Vycor/Gelsil sample due to capillarity (Fig. 9). After filling until saturation, the sample is cooled down to 170 K again (Fig. 10). The time dependence of the filling process is displayed in Fig. 9 for Vycor. While salol is percolating the sample, the temperature is held constant and the sample's height is measured. Charts for Gelsil 5.0 nm and Gelsil 2.6 nm look very similar. The diagrams in all cases show the typical $\sqrt{t}$ behavior as expected for a single capillary rise experiment, following Lucas[55] and Washburn.[56] This result is in concordance with findings of Huber *et al.*,[57] who investigated the mass uptake of porous silica samples and its time dependence, leading to the Lucas-Washburn $\sqrt{t}$ behavior of the mass uptake with time. Very recently it was shown that the Lucas-Washburn equation (with small modifications) works well even at the nanoscale,[58] which is in harmony with our results.

The expansion of a porous sample during adsorption of gases or water has already been investigated in the 1920s.[59] As a liquid/gas intrudes the sample it is subject to a negative hydrostatic pressure inside the pores, which leads to an expansion of the porous sample during adsorption of gases or water. Mesoporous media have enormous inner surfaces up to some 100 m^2/g (see Table I). This leads to a considerable stress reduction within the whole matrix and a sudden voluminal growth, which slows down and stops as all pore space is filled (see Fig. 9). The change in height due to the adsorption swelling can even be calculated quantitatively. The pressure reduction of the liquid in a capillary is known[60] as $P_c=2\sigma/r$, with the surface tension σ and the capillary radius r. With $\sigma=1.73\times10^{-2}$ N/m from Ref. 28, this yields a capillary pressure of 26.6 MPa in 2.6 nm pores. This would lead to a hypothetical capillary rise of 1.8 km for salol. The linear strain $\epsilon=\Delta h/h$ accompanying the filling process can be computed by the equation[61]

$$\epsilon=\frac{f\cdot P_c}{3}\left(\frac{1}{K}-\frac{1}{K_s}\right) \tag{6}$$

with the filling fraction f, the bulk modulus K of the empty host matrix, and the bulk modulus of the material building

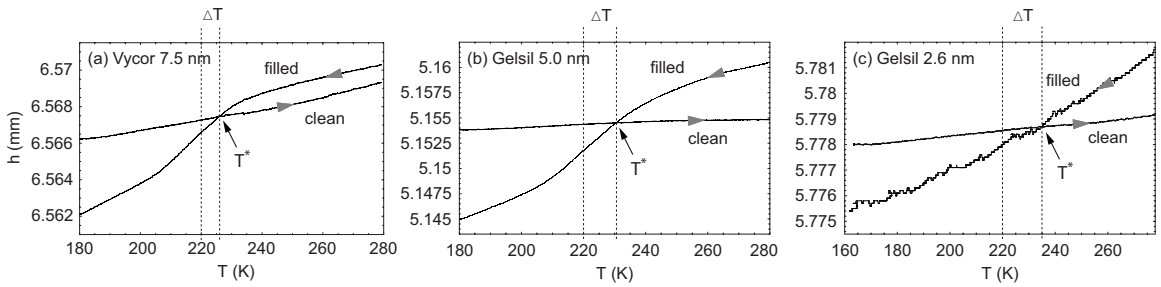

FIG. 10. Linear thermal expansion of empty and salol filled samples with pore diameters of (a) 7.5 nm, (b) 5.0 nm, and (c) 2.6 nm.

TABLE III. Variables of Eq. (6).

	Vycor	Gelsil 5	Gelsil 2.6
d (nm)	7.5	5.0	2.6
Porosity Φ	0.31	0.66	0.51
P_c (MPa)	9.2	13.8	26.6
K (GPa)	8.1	3.9	9.6
f	0.77	0.62	0.32
ϵ_{calc}	2.3×10^{-4}	6.6×10^{-4}	2.2×10^{-4}
ϵ_{exp}	1.0×10^{-4}	4.1×10^{-4}	3.5×10^{-4}

the solid frame K_s (which is nearly pure SiO_2). The bulk moduli K have been determined by RUS.[62] Table III shows parameters used to calculate $\epsilon=\Delta h/h$. The calculated values for the adsorption swelling agree rather well with the experimental results.

C. Negative pressure effect

The downshift of the glass transition in nm-confining pores is often reported to obey a $1/d$ law (see Refs. 23, 25, 28, and 63). At first this was proposed by Jackson and McKenna,[23] following their former results on the shift of the melting transition T_m in confinement.[64] But the supposed suppression of molecular cooperation when the pore diameter approaches an inherent length scale is not the only possible reason for a downward shift of T_g in confinement. Zhang *et al.*[63] proposed the increase in negative hydrostatic pressure within the pores due to mismatching thermal expansions of liquid and host matrix as the main driving force for the downshift of T_g. This idea was also discussed by Patkowski *et al.*[28] and Simon *et al.*,[65] and was reviewed by Alcoutlabi and McKenna.[34]

As Fig. 10(a) shows, for large pores and in a cooling process starting at RT, at higher temperatures the Vycor matrix is not affected by its filling. It contracts like the empty Vycor matrix with a thermal expansion coefficient $\alpha=\Delta h/(h\cdot\Delta T)=5.1\times10^{-6}$ K^{-1}. Patkowski *et al.*[28] proposed the possible flow and equilibration of the confined liquid well above T_g, which we also consider to be the case here. But as vitrification sets in at about 230 K, the filled Vycor matrix is subject to a contraction which is stronger compared to the empty Vycor sample. Strong interaction (H bondings) between salol and the pore surface might be the reason for this. At smaller pores of filled Gelsil samples [Figs. 10(b) and 10(c)] additional contraction already starts at higher temperatures. For an estimation of the process developing negative pressure upon the filling liquid, the strain misfit between the glass and the host matrix is

$$\Delta\epsilon^{mf}=3(\alpha_1-\alpha_2)\Delta T \tag{7}$$

with α_i, the thermal expansion coefficients of the host matrix (1) and salol (2). Negative pressure then derives from $\Delta P=\Delta\epsilon/\kappa_T$, where κ_T is the bulk compressibility of salol. The resulting shift of T_g, i.e.,

TABLE IV. Parameters of ΔT_g estimations, $\Delta T_g^{\text{exp}}=\Delta T_g^{np}+\Delta T_g^{\text{conf}}$.

	Vycor	Gelsil 5.0	Gelsil 2.6
d (nm)	7.5	5.0	2.6
α_2 (K^{-1})	2.1×10^{-5}	4.6×10^{-5}	1.1×10^{-5}
ΔT (K)	6	10	15
$\Delta\epsilon^{mf}$ (%)	−0.40	−0.60	−1.06
ΔP (MPa)	−8.1	−12.0	−21.1
ΔT_g^{np} (K)	−1.6	−2.4	−4.3
ΔT_g^{conf} (K)	−1.4	−2.9	−6.4
ΔT_g^{exp} (K)	−3.0	−5.3	−10.7

$$T_g(P)=T_g(P=0)\cdot\left.\frac{\partial T_g}{\partial P}\right|_{P=0}\cdot\Delta P \tag{8}$$

crucially depends on the choice of ΔT, the temperature range, in which the effective negative pressure upon salol develops. This effective temperature range can be estimated from our data as follows: As calculated from Eq. (6) the host porous matrix expands with filling due to the negative capillary pressure which acts on the confined liquid. Since with cooling the liquid salol contracts, this stress relaxes and the composite is stress free if the filled sample height is the same as for the empty matrix which occurs at $T=T^*$ (see Fig. 10). So $\Delta T\approx T^*-T_g$. Results of these estimations are given in Table IV. Parameters used for salol are $\kappa_T=5\times10^{-10}$ Pa^{-1} from Ref. 66, the thermal expansion coefficient $\gamma_1=3\alpha_1=7.36\times10^{-4}$ K^{-1} from Ref. 1, and $\partial T_g/\partial P=0.204$ K/MPa from Ref. 67. Our measurements are in accordance with enthalpy recovery results of Simon *et al.*[65] Their model shows that effective negative pressure develops 2 to 2.5 K above the reduced glass transition for samples with 11.6 and 25.5 nm pore sizes. Further, they state "…If negative pressure were the cause of the depressed T_g, the temperature at which isochoric conditions are imposed would have to be ~20 to 40 K above T_g." For comparison we obtain a necessary $\Delta T=10$ to 40 K for $d=7.5$ to 2.6 nm pores, which is in very good agreement with Simon *et al.*

In our opinion our calculated ΔT_g^{np} is still overestimated for two reasons: First, using the bulk value α_2 of the host matrix from Fig. 10 does not take into account internal pore walls being affected by the negative pressure inside, relaxing to some extent and so reducing pressure. Second, thermal expansions of other glass forming liquids, e.g., toluene have been reported 1.5 times smaller in confinement[68] compared to bulk. Moreover, thermal expansion of liquid salol drops[1] to a *quarter* of its value at the glass transition. So, as the glass transition sets in, α_1 starts to decrease and a purely pressure induced downshift ΔT_g would be even more diminished. Apart from this the reason for the size dependence of the thermal mismatch effect (see Fig. 11, open circles) is not clear at all.

IV. CONCLUSIONS

The glass transition of salol confined to porous host matrices of Vycor and Gelsil with pore sizes of 7.5, 5.0 and 2.6

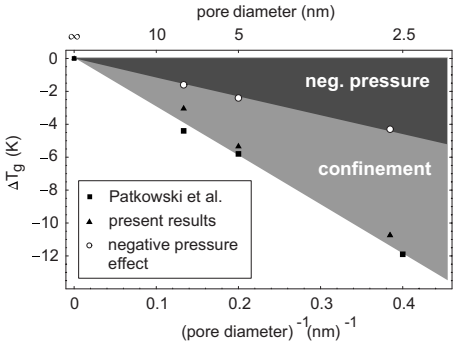

FIG. 11. Shift of glass transition temperature against (pore diameter)$^{-1}$. The boxes are T_g's from Fig. 8, triangles show literature values from Ref. 28, and open circles display the maximum negative pressure contribution (see Sec. III C).

nm has been measured by Dynamic Mechanical Analyzers (DMA 7 and Diamond DMA, Perkin Elmer). The dynamic complex elastic susceptibility data can well be fitted assuming two types of dynamic processes: A "bulk" relaxation in the core of the pores and a radially increasing "surface relaxation" of molecules near the pore surface. The calculated core relaxation time shows a typical Vogel-Fulcher temperature dependence and decreases with decreasing pore size d. This confinement induced acceleration of dynamics leads to a shift of the glass transition temperature $T_g \propto 1/d$, which is in perfect agreement with recent DSC results.[28] Measurements of the sample height with filling (adsorption swelling) and thermal expansion are used to calculate the effect of "negative pressure" due to thermal mismatch between the porous host matrix and the glass forming liquid. Such negative pressure could at least partly explain a shift of T_g in confined glass forming liquids.[28,34,65] Our data show that for salol this effect of thermal mismatch could describe at most 30% of the observed downshift of T_g, which is in harmony with enthalpy recovery experiments.[65]

In our opinion the main cause for the shift of T_g is a hindering of cooperativity due to confinement. This is also supported by an estimation of this effect using the results of Hunt *et al.*[69] They calculated the finite-size effect of the glass transition from percolation and effective medium models, which yields

$$T_g(d) = T_g(\text{bulk}) - \frac{0.5 \cdot E}{\ln(t \cdot \nu_{\text{ph}})} \cdot \frac{r_0}{L}. \tag{9}$$

Inserting $t=100$ s, $\nu_{\text{ph}}=1/\tau_0$, and our fit parameters from Table II, and assuming that the typical distance between molecules r_0 is about the diameter of a salol molecule[52] ($d_0 \approx 0.8$ nm), we obtain ΔT_g^{Hunt} as 3.2, 4.8 and 9.1 K for 7.5, 5.0 and 2.6 nm pores, respectively. These calculated values agree surprisingly well with the measured confinement induced downshifts of $T_g(d)$ (see Fig. 11 and ΔT_g^{exp} in Table IV).

Moreover Eq. (9) predicts[69] that the size dependence of ΔT_g increases with increasing fragility,[70]

$$m = \frac{E \cdot T_g}{\ln(10)(T_g - T_0)^2}, \tag{10}$$

since $m \propto E$. Indeed, this correlation between $\Delta T_g(d) \sim m$ was verified experimentally for many systems, i.e., for glycerol[63] ($m=53$) ΔT_g ($d=2.5$ nm) ≈ -4 K, benzyl-alcohol[23] ($m=65$) ΔT_g ($d=2.5$ nm) ≈ -9 K, salol[28] ($m=73$) ΔT_g ($d=2.5$ nm) ≈ -11 K, o-terphenyl[28] ($m=81$) ΔT_g ($d=2.5$ nm) ≈ -25 K.

We think that these considerations, i.e., the downshift of T_g calculated via percolation theory, as well as the clear correlation between the magnitude of induced T_g shift and the fragility of a glass forming liquid, both confirm our other findings (see Fig. 11) that the main effect of the confinement is to suppress cooperative motion. Negative pressure effects although always present contribute only little.

ACKNOWLEDGMENTS

Support by the Austrian FWF (Grant No. P19284-N20) and by the University of Vienna within the IC Experimental Materials Science ("Bulk Nanostructured Materials") is gratefully acknowledged. We thank Marie-Alexandra Neouze and the Institute of Materials Chemistry from the Vienna University of Technology for the N_2-characterization of our samples. We are grateful to J. Bossy (CNRS Grenoble) for supplying us with Gelsil samples.

*johannes.koppensteiner@univie.ac.at
†wilfried.schranz@univie.ac.at
‡madalina-roxana.puica@univie.ac.at

[1] M. Cukiermann, J. W. Lane, and D. R. Uhlmann, J. Chem. Phys. **59**, 3639 (1973).
[2] M. D. Ediger, C. A. Angell, and S. R. Nagel, J. Phys. Chem. **100**, 13200 (1996).
[3] W. Kauzmann, Chem. Rev. (Washington, D.C.) **9**, 219 (1948).
[4] G. Adam and J. H. Gibbs, J. Chem. Phys. **43**, 139 (1965).
[5] J. Jäckle, and A. Krönig, J. Phys.: Condens. Matter **6**, 7633 (1994).
[6] C. Donati, J. F. Douglas, W. Kob, S. J. Plimpton, P. H. Poole, and S. C. Glotzer, Phys. Rev. Lett. **80**, 2338 (1998).
[7] C. Bennemann, C. Donati, J. Baschnagel, and S. C. Glotzer, Nature (London) **399**, 246 (1999).
[8] P. Scheidler, W. Kob, K. Binder, and G. Parisi, Philos. Mag. B **82**, 283 (2002).
[9] G. Biroli, J.-P. Bouchaud, K. Miyazaki, and D. R. Reichmann, Phys. Rev. Lett. **97**, 195701 (2006).
[10] E. Hempel, G. Hempel, A. Hensel, C. Schick, and E. Donth, J. Phys. Chem. B **104**, 2460 (2000).
[11] E. Donth, H. Huth, and M. Beiner, J. Phys.: Condens. Matter **13**, L451 (2001).
[12] U. Tracht, M. Wilhelm, A. Heuer, H. Feng, K. Schmidt-Rohr, and H. W. Spiess, Phys. Rev. Lett. **81**, 2727 (1998).
[13] S. A. Reinsberg, A. Heuer, B. Doliwa, H. Zimmermann, and H.

W. Spiess, J. Non-Cryst. Solids **307-310**, 208 (2002).
[14] X. H. Qiu and M. D. Edinger, J. Phys. Chem. B **107**, 459 (2003).
[15] L. Berthier, G. Biroli, J.-P. Bouchard, L. Cipelletti, D. El Masri, D. L'Hote, F. Ladieu, and M. Pierno, Science **310**, 1797 (2005).
[16] R. Bergman and J. Swenson, Nature (London) **403**, 283 (2000).
[17] J. C. Dore, M. Dunn, T. Hasebe, J. H. Strange, and M. C. Bellissent-Funel, Springer Proc. Phys. **37**, 144 (1989).
[18] V. P. Soprunyuk, D. Wallacher, P. Huber, K. Knorr, and A. V. Kityk, Phys. Rev. B **67**, 144105 (2003).
[19] P. Huber and K. Knorr, *Nanoporous and Nanostructured Materials for Catalysis, Sensor and Gas Separation Applications*, MRS Symposia Proceedings No. 876E (Materials Research Society, Pittsburgh, 2005), p. R3.1.
[20] G. S. Iannacchione, G. P. Crawford, S. Qian, J. W. Doane, D. Finotello, and S. Zumer, Phys. Rev. E **53**, 2402 (1996).
[21] A. V. Kityk, T. Hofmann, and K. Knorr, Phys. Rev. Lett. **100**, 036105 (2008).
[22] Eur. Phys. J. E **12**, 3 (2003), special issue on dynamics in confinement, edited by B. Frick, M. Koza, and R. Zorn.
[23] C. L. Jackson and G. B. McKenna, J. Non-Cryst. Solids **131-133**, 221 (1991).
[24] A. Schönhals, H. Göring, C. Schick, B. Frick, and R. Zorn, Colloid Polym. Sci. **282**, 882 (2004).
[25] O. Trofymluk, A. A. Levchenko, and A. Navrotsky, J. Chem. Phys. **123**, 194509 (2005).
[26] R. Kremer, A. Huwe, A. Schönhals, and A. S. Rzanski, *Molecular Dynamics in Confining Space in Broadband Dielectric Spectroscopy*, edited by F. Kremer and A. Schönhals (Springer-Verlag, Berlin, 2000), p. 171.
[27] R. Zorn, L. Hartmann, B. Frick, D. Richter, and F. Kremer, J. Non-Cryst. Solids **307**, 547 (2002).
[28] A. Patkowski, T. Ruths, and E. W. Fischer, Phys. Rev. E **67**, 021501 (2003).
[29] P. Scheidler, W. Kob, and K. Binder, Europhys. Lett. **52**, 277 (2000).
[30] H. Sillescu, J. Non-Cryst. Solids **243**, 81 (1999).
[31] E. Donth, *The Glass Transition* (Springer-Verlag Heidelberg, 2001).
[32] K. Kim and R. Yamamoto, Phys. Rev. E **61**, R41 (2000).
[33] S. Karmakar, C. Dasgupta, and S. Sastry, arXiv:0805.3104 (unpublished).
[34] M. Alcoutlabi and G. B. McKenna, J. Phys.: Condens. Matter **17**, R461 (2005).
[35] C. Alba-Simionesco, B. Coasne, G. Dosseh, G. Dudziak, K. E. Gubbins, R. Radhakrishnan, and M. Sliwinska-Bartkowiak, J. Phys.: Condens. Matter **18**, R15 (2006).
[36] W. Schranz, M. R. Puica, J. Koppensteiner, H. Kabelka, and A. V. Kityk, Europhys. Lett. **79**, 36003 (2007).
[37] P. Scheidler, W. Kob, and K. Binder, Europhys. Lett. **59**, 701 (2002).
[38] T. H. Elmer, *Engineered Materials Handbook* (ASM International, Materials Park, OH, 1992), Vol. 4, p. 427.
[39] P. Levitz, G. Ehret, S. K. Sinha, and J. M. Drake, J. Chem. Phys. **95**, 6151 (1991).
[40] F. Rouguerol, J. Rouguerol, and K. Sing, *Adosorption by Powders and Porous solids: Priciples, Methodology and Applications* (Academic, New York, 1999).
[41] T. Scopigno, G. Ruocco, F. Sette, and G. Monaco, Science **302**, 849 (2003).
[42] W. Schranz, Phase Transitions **64**, 103 (1997).
[43] W. Schranz and D. Havlik, Phys. Rev. Lett. **73**, 2575 (1994).
[44] K. P. Menard, *Encyclopedia of Chemical Processing* (Taylor and Francis, London, 2006), p. 799.
[45] W. Gorbatschow, M. Arndt, R. Stannarius, and F. Kremer, Europhys. Lett. **35**, 719 (1996).
[46] P. Pissis, A. Kyritsis, D. Daoukaki, G. Barnt, R. Pelster, and G. Nimtz, J. Phys.: Condens. Matter **10**, 6205 (1998).
[47] D. A. Sappelt and J. Jäckle, J. Phys. A **26**, 7325 (1993).
[48] P. Scheidler, W. Kob, and K. Binder, Eur. Phys. J. E **12**, 5 (2003).
[49] M. Arndt, R. Stannarius, H. Groothues, E. Hempel, and F. Kremer, Phys. Rev. Lett. **79**, 2077 (1997).
[50] F. Kremer and R. Stannarius, Lect. Notes Phys. **634**, 275 (2004).
[51] A. G. Kalampounias and S. N. Yannopoulos, J. Chem. Phys. **118**, 8340 (2003).
[52] E. Eckstein, J. Qian, R. Hentschke, T. Thurn-Albrecht, W. Steffen, and E. W. Fischer, J. Chem. Phys. **113**, 4751 (2000).
[53] R. Richert and C. A. Angell, J. Chem. Phys. **108**, 9016 (1998).
[54] G. Diezemann and K. Nelson, J. Phys. Chem. B **103**, 4089 (1999).
[55] R. Lucas, Kolloid-Z. **23**, 15 (1918).
[56] E. W. Washburn, Phys. Rev. **17**, 273 (1921).
[57] P. Huber, S. Grüner, C. Schäfer, K. Knorr, and A. V. Kityk, Eur. Phys. J. Spec. Top. **141**, 101 (2007).
[58] D. I. Dimitrov, A. Milchev, and K. Binder, Phys. Rev. Lett. **99**, 054501 (2007).
[59] F. T. Meethan, Proc. R. Soc. London, Ser. A **15**, 223 (1927).
[60] L. D. Landau and E. M. Lifshitz, in *Course of Theoretical Physics*, edited by G. Heber, (Akademieverlag, Berlin, 1996), Vol. VI.
[61] D. P. Bentz, E. J. Garboczi, and D. A. Quenard, Modell. Simul. Mater. Sci. Eng. **6**, 211 (1998).
[62] J. Koppensteiner, M. A. Carpenter, and W. Schranz, (unpublished).
[63] J. Zhang, G. Liu, and J. Jonas, J. Phys. Chem. **96**, 3478 (1992).
[64] C. L. Jackson and G. B. McKenna, J. Chem. Phys. **93**, 9002 (1990).
[65] S. L. Simon, J.-Y. Park, and G. B. McKenna, Eur. Phys. J. E **8**, 209 (2002).
[66] H. Kamioka, Jpn. J. Appl. Phys., Part 1 **32**, 2216 (1993).
[67] R. Casalini, M. Paluch, and C. M. Roland, J. Phys. Chem. A **107**, 2369 (2003).
[68] D. Morineau, Y. D. Xia, and C. Alba-Simionesco, J. Chem. Phys. **117**, 8966 (2002).
[69] A. Hunt, Solid State Commun. **90**, 527 (1994).
[70] R. Boehmer, K. L. Ngai, C. A. Angell, and D. J. Plazek, J. Chem. Phys. **99**, 4201 (1993).